Design and optimization of a spectrometer for Spectral Domain Optical Coherence Tomography

Hamid Hosseiny*[a,b], Carla Carmelo Rosa[a,b]
[a]INESC Porto, Rua do Campo Alegre 687, 4169-007 Porto, Portugal
[b]Departamento de Física e Astronomia, Faculdade de Ciências da Universidade do Porto, Rua do Campo Alegre 687, 4169-007 Porto, Portugal

ABSTRACT

There are several factors such as the chosen optical source, central wavelength, spectral bandwidth, spectrometer optical components and the detector specifications that affect the overall performance of a spectral domain optical coherence tomography (SD-OCT) imaging system. Among these factors a good design and implementation of the spectrometer is of paramount importance as it directly affects the system resolution, sensitivity fall-off, maximum imaging depth, SNR and in general the system performance. This study demonstrates the design steps and some considerations during the design of a spectrometer. The imaging performance of this design is assessed. The obtained experimental results prove an improvement of the overall performance of the common path SD-OCT imaging system and agree with the expected outcome from the design stage.

Keywords: Spectrometer design and optimization, Spectral domain optical coherence tomography, Common path spectral domain optical coherence tomography

*H.Hosseiny@fc.up.pt; phone 351 220 901 945; fax 351 220 402 437; fc.up.pt

1. INTRODUCTION

The spectrometer used in spectral domain optical coherence tomography (SD-OCT) imaging system is a critical component playing an important role in obtaining high quality OCT images. The optical interference signal is captured by a spectrometer placed at the detection arm of the OCT interferometer. A typical spectrometer consists of collimating optics, a diffraction grating, focusing optics and a line-scan detector. The depth profile, known as A-scan, is measured by taking an inverse Fourier transform from a single spectrum acquired without any need for mechanical movements of the reference mirror [1]. Using a line-scan detector and keeping the reference arm fixed allow faster acquisitions of A-scans [2]. This minimizes distortion and artifacts introduced by sample motion in OCT images. The other benefits of this technique are high sensitivity and signal to noise ratio advantages over the conventional time domain optical coherence tomography (TD-OCT) [3].

So far various spectrometer designs have been proposed for SD-OCT imaging system. Hu et al. presented a linear-in-wavenumber spectrometer employing a prism after the diffraction grating to linearize the spectrum data in wavenumber [4]. This hardware design approach eliminates numerical interpolation, decreases computational processing time and improves the depth dependent sensitivity fall-off. Kamal et al. proposed an all-reflective optics spectrometer consisting of a fold mirror, a grating, a cylindrical mirror and a line-scan detector in order to eliminate the chromatic aberration and increase the image quality [5]. In contrast, there are other conventional and commonly used spectrometers employing refractive optics-based components [6, 7]. These optical spectrometer components are normally installed in free space, and are bulky. Akca et al. demonstrated a silicon-oxynitride based arrayed waveguide grating (AWG) spectrometer to reduce the size of the bulky free-space spectrometer [8]. They fabricated an AWG and integrated into the spectrometer of a SD-OCT system for spectral bandwidth of 800 nm – 1300 nm.

Second International Conference on Applications of Optics and Photonics, edited by Manuel Filipe P. C. Martins Costa, Rogério Nunes Nogueira, Proc. of SPIE Vol. 9286, 92864Z · © 2014 SPIE · CCC code: 0277-786X/14/$18 · doi: 10.1117/12.2063755

In this paper optical design steps for a spectrometer with a spectral bandwidth of 70 nm and central wavelength at 1050 nm is presented. The spectrometer is integrated into a common path SD-OCT imaging system. The imaging performance is characterized based on different specifications such as maximum imaging depth, axial resolution, depth dependent sensitivity fall-off, SNR, fringe visibility and temporal performance. The results are recorded and demonstrated. Three different samples are imaged in order to validate the quality of system improvement and also to measure the optical thickness of diverse layers.

2. METHOD

2.1 Spectrometer design steps

The spectrometer specification is identified at the initial stage of the spectrometer design. Spectrometer specification is determined by the optical source specification, the axial resolution and maximum imaging depth. The employed light source has wavelength bandwidth of 1015 – 1085 nm, centered approximately at 1050 nm. The axial resolution is specified by the coherence length of the light source. For a Gaussian spectrum the coherence length (l_c) is defined as follows:

$$\mathrm{l_c} = \frac{4\ln 2}{\pi}\frac{\lambda_0^2}{\Delta\lambda} \tag{1}$$

where λ_0 is the central wavelength and $\Delta\lambda$ is the full width at half maximum of the light source wavelength. Therefore, the minimum resolvable distance or in other words the axial resolution (Δz) is given by:

$$\Delta\mathrm{z} = \frac{\mathrm{l_c}}{2\mathrm{n}} = \frac{2\ln 2}{\mathrm{n}\pi}\frac{\lambda_0^2}{\Delta\lambda} \tag{2}$$

where n is the refractive index of the interrogated sample. Considering the given light source specification and equation (2), the calculated axial resolution in air is approximately 6.93 μm.

The maximum imaging depth is determined by the resolution of the spectrometer and is also limited by the scattering and absorption properties of the imaged object. The spectrometer resolution ($\delta\lambda$) and maximum imaging depth (Z_{max}) are given by:

$$\delta\lambda = \frac{\Delta\lambda}{\mathrm{N}} \tag{3}$$

$$\mathrm{Z_{max}} = \frac{\lambda_0^2}{4\mathrm{n}\,\delta\lambda} \tag{4}$$

where N is the total number of illuminated pixels at the line-scan detector. Assuming N = 1024 pixels, n = 1, the needed spectrometer resolution is calculated as 0.068 nm, and the maximum imaging depth is measured as 4032 μm ≈ 4 mm.

A typical SD-OCT spectrometer consists of four principal components: a collimator, a diffraction grating, a focusing lens and a line-scan camera detector. In the next step of the spectrometer design, the line-scan camera specification will be considered since the constraints at this stage would affect other spectrometer components. A commercial Dalsa SG-10-02K80-00-R Spyder3 GigE line-scan camera with 2048 pixels, pixel size of 14 μm ×14 μm with minimized space between pixels, was selected as it realizes the spectrometer resolution and also was available in the lab.

A prism or a grating can be employed to spectrally disperse the light over the detector. Gratings are normally used as they are less bulky and provide higher spectral resolution. The properties of the grating strongly influence the spectrometer resolution. Gratings are defined by their resolving power (R) which is a dimensionless number and is given by:

$$R = \frac{\lambda}{\delta\lambda} = mN \quad (5)$$

where $\delta\lambda$ is the maximum achievable spectral resolution of the grating, m is the diffraction order and N is the total number of grooves illuminated on the grating surface. Most gratings are first orders meaning, they are highly efficient at first diffraction order. Maximum wavelength is considered to calculate the resolving power. Assuming m = 1 and λ = 1085 nm, to realize $\delta\lambda$ = 0.068 nm the total number of illuminated grooves is obtained as 15,956. Therefore, if a groove density of 1200 mm^{-1} is chosen, the beam diameter or in other words the minimum aperture size for the collimating lens must be at least 13.3 mm. In an attempt to determine the collimating lens, the angle at which the light exits the fiber (β) is first measured. The angle depends on the numerical aperture (NA) of the fiber and refractive index of the medium through which the light travels.

$$NA = n\,Sin(\beta) \quad (6)$$

The numerical aperture of the used fiber is 0.13 and as the light exits the fiber into the air (n = 1), hence β is obtained as 7.5 degrees. Using a simple geometry formula, the focal length for the collimating lens is estimated as ~50.5 mm. However, an achromatic doublet lens with the focal length of 75 mm was selected, further expanding the beam without damage to the spectrometer resolution.

For the selection of a grating the next issue that should be taken into account is the efficiency. Grating efficiency is a function of wavelength and polarization of the incident light. Considering the computed beam diameter and the efficiency plot of the gratings, a ruled diffraction grating of 1200 grooves/mm with the size of 25 mm × 25mm was chosen. After the grating selection, the next step is to determine the angular dispersion of the grating that is given as follows:

$$Sin\theta_i + Sin\theta_d = mG\lambda \quad (7)$$

where Θ_i is the incident angle of the light, Θ_d is the dispersion angle, m is the diffraction order and G is the groove density. Assuming m = 1 and G = 1200 mm^{-1}, the dispersion angle for minimum, central and maximum wavelength is obtained as 36^o, 39^o and 42^o respectively. Therefore, the spectrum from 1015 nm – 1085 nm is dispersed by the grating at Θ_d = 39^o with the dispersion angle of ±3 degrees. Applying Littrow condition (Θ_i = Θ_d), the optimal efficiency is achieved at 39^o, hence the grating is placed at close to Littrow angle.

A 2-inch achromatic doublet lens with the focal length of 80 mm was considered for the focusing lens. As the last step, the camera was placed on a customized x-y-z stage controller at the focal distance of the focusing lens to better control the camera position in order to obtain maximum possible signal.

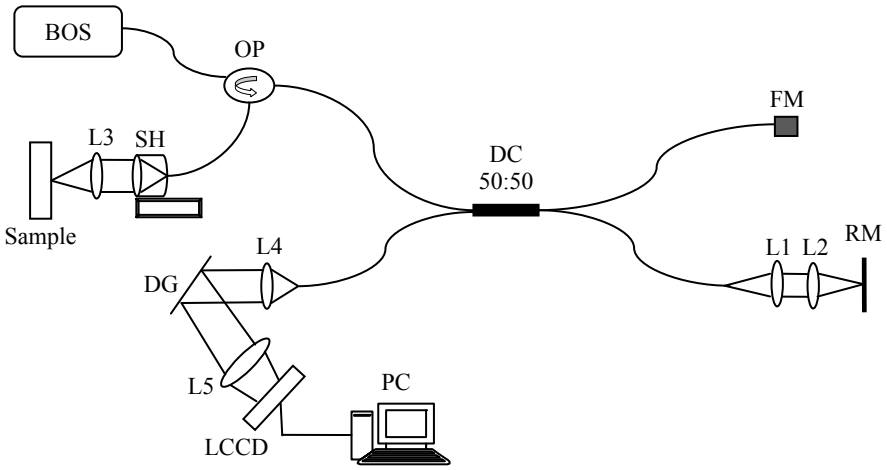

Figure 1. Schematic diagram of the common path SD-OCT imaging system. BOS: Broadband Optical Source, OP: Optical Circulator, SH: Sensing Head installed on a motorized stage controller, DC: 50/50 Directional Coupler, FM: Fiber optic Mirror, RM: Reference Mirror, DG: Diffraction Grating, LCCD: Line-scan Charge Coupled Device camera, PC: Personal Computer and L1-5: Achromatic Lenses.

2.2 System setup

A schematic diagram of the common path SD-OCT system is shown in Figure 1. The light is emitted from a Multiwave Photonics' Broadband ASE source with spectral width of 70 nm, central wavelength at 1050 nm, and output power of 20 mW. It passes through an optical coupler. A FC/PC fiber connector is utilized to connect the fiber to the sensing head such that a fraction of light returns and the rest travels through the sample. The sensing head is installed on a motorized positioning stage controller. Back scattered and back reflected light pass through a 50/50 fiber optic directional coupler and undertake interference if the optical path at both reference arms are matched. Finally the interfering light is detected by the spectrometer. The spectrometer comprises of an achromatic doublet collimating lens (shown as L4 in Figure 1), a ruled diffraction grating of 1200 grooves/mm and an achromatic doublet focusing lens (L5) to image the entire spectral bandwidth to a line-scan charge coupled device camera (LCCD). The used LCCD is Dalsa SG-10-02K80-00-R Spyder3 GigE line-scan camera with the line rate of 36 kHz and total number of pixels of 2048 that each pixel size is 14 μm ×14 μm. The data collected by the camera is ultimately transferred to a PC via an Ethernet card.

3. RESULTS

After installation of the spectrometer components, the common path SD-OCT system performance was characterized considering different specifications. These performance specifications include maximum imaging depth, axial resolution, fringe visibility, sensitivity fall-off, signal to noise ratio and processing time. The system was first calibrated using the spectral calibration technique reported in our earlier publication [9]. The maximum imaging depth was measured by placing a flat mirror in the sample arm and translating the sensing head with the step of 50 μm while the reference mirrors are fixed. The maximum imaging depth of 3.1 mm was achieved. The theoretical system axial resolution was calculated as 6.93 μm in air. The fringe visibility of 38% was acquired at the optical path difference (OPD) close to zero. 512 A-scans at 16 different OPDs were captured to measure the sensitivity fall-off. The camera exposure time and line rate for each A-scan are 27 μs and 36 kHz respectively. The interference fringes were processed using the developed signal processing algorithm proposed in the previous study [10]. The sensitivity fall-off of -22.42 dB was obtained at maximum imaging depth. SNR at various OPDs was measured and plotted in Figure 2. The SNR was calculated by $20\log_{10}(R_s/R_n)$ where R_s indicates the highest amplitude of the signal and R_n indicates the root mean square of the noise. The temporal performance was computed. For the images with the size of 512 × 1024, graphics processing unit (GPU)

processing time for the entire signal processing steps was approximately 17 ms, and if the data acquisition time and ensemble averaging execution time run by central processing unit (CPU) added, the total processing time for 512 A-lines would be 76 ms. In overall the data processing speed of the system was approximately 6.73k A-lines/s.

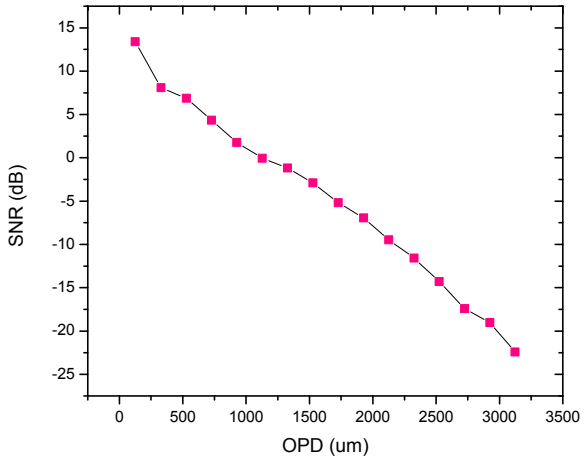

Figure 2. The common path SD-OCT system SNR measurement ($\Delta\lambda$ = 70 nm and Z_{max} = 3.1 mm)

After system performance characterization, three different samples were imaged. First a plain glass microscope slide with the thickness of approximately 1 mm was tested. The glass microscope slide has the refractive index of 1.5251. The resulting depth profile shown in Figure 3 demonstrates two reflections obtained from the front and the back surface of the glass slide. As it can be seen, the optical thickness of 1537 μm was obtained, confirming the physical thickness of the sample under test.

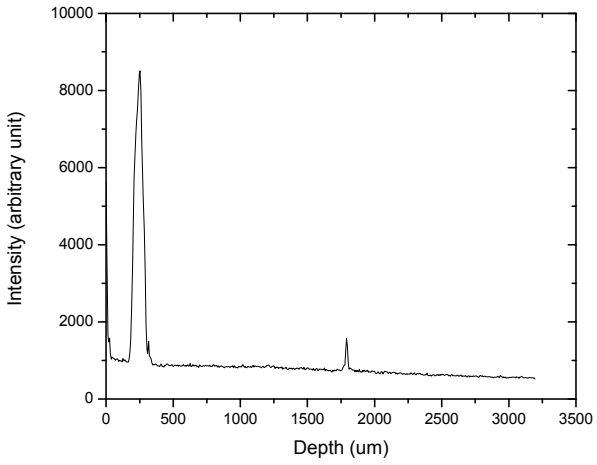

Figure 3. The depth profile of the imaged glass slide. The distance between two peaks is 1537 μm, proving the physical thickness (1mm) of the glass slide.

The next sample was a very thin film sandwiched between two glass slides. Each glass slide has the physical thickness of 1 mm, and the physical thickness of the thin film is within the range of 100 μm – 300 μm. The resulting depth profile illustrated in Figure 4 shows four reflections obtained from the front and the back surface of the first glass slide (the peaks labeled as 1 and 2), and the front and the back surface of the thin interior film (the peaks labeled as 3 and 4). The first peak with no label in the beginning of the depth profile is the coherence noise. The distance between peak 1 and 2 is 1620 μm, demonstrating the optical distance of the first glass slide. The distance between peak 3 and 4 is 234 μm,

showing the optical distance of the thin film. As it is illustrated in Figure 4, there is air between the first glass slide and the thin film. This gap is measured as 95 μm.

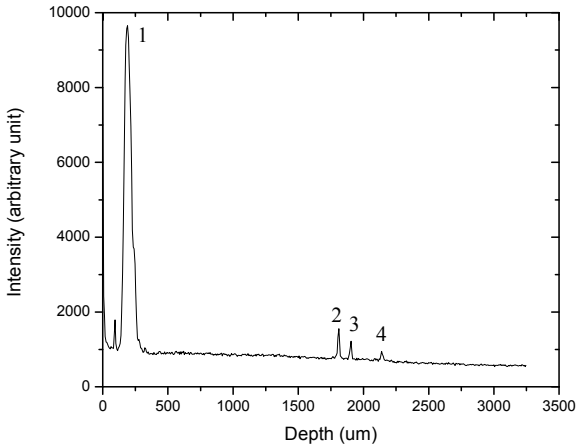

Figure 4. The depth profile of a very thin film sandwiched between two plain glass slides. The optical distance between peak 1 and 2 is 1620 μm, and the optical distance between peak 3 and 4 is 234 μm. There is air between the first glass slide and the thin film which measured as 95 μm (the optical distance between peak 2 and 3).

In the next attempt a polyethylene terephthalate (PET) preform, which its structure explained in our previous study, was used as an object [10]. The very thin film inside the preform was imaged. Figure 5 shows the depth profile of the film demonstrating two reflections acquired from the front and the back surface of the film. As the film is very thin, and there is significant scattering effect, more than one peak was obtained at the first reflection of the thin film. These peaks are labeled as 1 in Figure 5. The optical distance between two peaks labeled as 1 and 2 was measured as 456 μm.

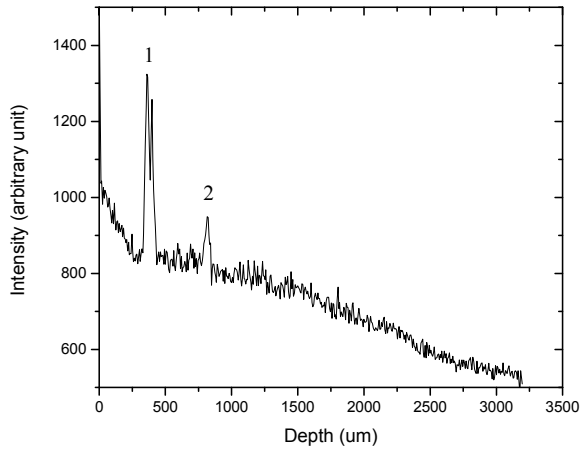

Figure 5. The depth profile of a thin film inside a PET preform, demonstrating two reflections obtained from the front and the back surface of the film. The optical distance between the peaks labeled as 1 and 2 is approximately 456 μm.

4. CONCLUSIONS

In the present study the necessary steps and some considerations to design a spectrometer for the SD-CP-OCT imaging system were explained. After spectrometer's components installation, the system was characterized based on some system performance specifications such as: maximum imaging depth, axial resolution, fringe visibility, sensitivity fall-off, SNR and processing time. These results were shown and evaluated. Three various samples were imaged. The aim was to validate the quality of system improvement and also to measure the optical thickness of diverse layers. In general the experimental results demonstrated an improvement in overall performance of the SD-CP-OCT system.

5. ACKNOWLEDGEMENTS

This work is funded by National Funds through the FCT – Fundação para a Ciência e a Tecnologia (Portuguese Foundation for Science and Technology), grant SFRH/BD/72801/2010.

6. REFERENCES

1. Fercher, A.F., *Optical coherence tomography – development, principles, applications.* Zeitschrift für Medizinische Physik, 2010. **20**(4): p. 251-276.
2. Wojtkowski, M., *High-speed optical coherence tomography: basics and applications.* Appl. Opt., 2010. **49**(16): p. D30-D61.
3. Leitgeb, R., C. Hitzenberger, and A. Fercher, *Performance of fourier domain vs. time domain optical coherence tomography.* Optics Express, 2003. **11**(8): p. 889-894.
4. Hu, Z. and A.M. Rollins, *Fourier domain optical coherence tomography with a linear-in-wavenumber spectrometer.* Optics Letters, 2007. **32**(24): p. 3525-3527.
5. Kamal, M., N. Sivakumar, and M. Packirisamy. *Design of a spectrometer for all-reflective optics-based line scan Fourier domain optical coherence tomography*. in *Photonics North 2010*. 2010.
6. Xi, P., et al., *Evaluation of spectrometric parameters in spectral-domain optical coherence tomography.* Applied Optics, 2011. **50**(3): p. 366-372.
7. Kamal, M., S. Narayanswamy, and M. Packirisamy. *Design of spectrometer for high-speed line field optical coherence tomography*. in *Photonics North 2011*. 2011.
8. Akca, B.I., et al. *Integrated Spectrometers for Spectral-Domain Optical Coherence Tomography*. in *CLEO/Europe and EQEC 2011 Conference Digest*. 2011. Munich: Optical Society of America.
9. Hosseiny, H. and C. Carmelo Rosa, *Numerical study on spectral domain optical coherence tomography spectral calibration and re-sampling importance.* Photonic Sensors, 2013. **3**(1): p. 35-43.
10. Hosseiny, H., et al. *Characterization of PET preforms using spectral domain optical coherence tomography*. in *8th Ibero American Optics Meeting/11th Latin American Meeting on Optics, Lasers, and Applications*. 2013: International Society for Optics and Photonics.